International Journal of Engineering Technology and Applied Science

(ISSN: 2395 3853), Vol. 3 Issue 5 May 2017

Micro-Structural Characterization of (TiB+TiC)/Ti6Al4V Material

[1]Lokesh Choudhary, [2]Dr. S. S. Chouhan, [3]Ranjeet Kumar
[1]M-Tech Scholar, [2]Director, [3]Professor
[123]Department of Mechanical Engineering, VITS, Bhopal, India

Abstract- In the paper the Simulation were carried out for the analysis of the Ti6Al4V composite were successfully indirect different extrusion angles of die in FEM processed (45°, 60° and75°). Initial compression stage, in which the load gradually increases, forms a small indentation hole by backward extrusion. Second stage, in which radial extrusion formation of billets are formed along with the forward extrusion of the part was performed, combined stage, corner die filling and extrusion of part was done, The unsteady state stage, in which there is a steep rise in load. In this stage, flash is formed, as the metal flow has hindered and controlled, the load increases unsteadily.

In case of third product metal flows out through the exit extrusion die present at the bottom, hence no flash provision is equipped. The last product is manufactured by multi stage extrusion process in which the first product is the initial input specimen. Hence, the process is thought consists of two stages.
In the present paper the finite element analysis for three different types of dies were performed by simulation processes. Similar conditions of experimental analysis are taken into account for performing the present FEM analysis. Combination of three types of dies with frictional conditions. Different stages of deformation for 45 degree dies are performed for clear understating of die filling. Different stages of die filling data are used for further comparison analysis. Different stages of metal flow pattern for 45 degree dies are obtained for clear understanding of grain flow and shear effected regions. Shows the punch load and punch displacement variation.

KEYWORDS: FEM, FEA, Punch Load. Die Angle, Die Filling

I INTRODUCTION

Microstructure is the small scale structure of a material, defined as the structure of a prepared surface of material as revealed by a microscope above 25× magnification. The microstructure of a material (such as metals, polymers, ceramics or composites) can strongly influence physical properties such as strength, toughness, ductility, hardness, corrosion resistance, high/low temperature behavior or wear resistance. These properties in turn govern the application of these materials in industrial practice. Microstructure at scales smaller than can be viewed with optical microscopes is often called nanostructure, while the structure in which individual atoms are arranged is known as crystal structure. The nanostructure of biological specimens is referred to as ultrastructure. A microstructure's influence on the mechanical and physical properties of a material is primarily governed by the different defects present or absent of the structure. These defects can take many forms but the primary ones are the pores. Even if those pores play a very important role in the definition of the characteristics of a material, so does its composition. In fact, for many materials, different phases can exist at the same time. These phases have different properties and if managed correctly, can prevent the fracture of the material.

II LITERATURE SURVEY

In 2016 Material and Science Engineering Wang Lu et al. [18] proposed Forged 5 vol. % (TiB+TiC)/Ti6Al4V titanium matrix composite billets with a heterogeneous reinforced structure was successfully hot indirect extruded with different dies angle($\theta = 45°$, 60° and 75°) at 1303 K. The dies angle was found to work as one key factor to change the micro structures and mechanical properties. Detail investigation on the micro structural evolution revealed that the significant grain refinement was obtained after extrusion due to dynamic recrystallization, the fully dynamic recrystallization takes place during indirect extrusion at dies angle 75°. In situ TiB and TiC reinforcements were also significantly refined by the indirect extrusion process, while highly developed preferred or mentation of TiB short fibers along extrusion direction. Meanwhile, the mechanical properties showed that the ultimate tensile strength, yield strength and elongation exhibited a simultaneous increase after the indirect extrusion, especially on the ductility of the materials. The strength was slightly improved but not too much by hot extrusion. However, both tensile strength and elongation to fracture were reduced as the extrusion dies angle enlarged from45° to 75°. Higher strength and elongation were obtained with optimal dies angle45°, confirmed by matrix refinement, dynamical recrystallization and the optimal aspect ratio of TiB short fibers. Therefore, the optimal hot extrusion with

the extrusion dies angle should be controlled less than 60°.

In 2017 Material Jian Lei Yang et al. [19] proposed that a novel extrusion with filler material to produce the high-performance TiBw/Ti-6Al-4V composite tube with a quasi-continuous reinforced structure. A simulation was adopted to study the effect of the filler material on the shape accuracy of the tubes. Based on the simulation results, the flow stress of the filler material was not the important factor, but the friction coefficient between the filler and TiBw/Ti-6Al-4V composite and the canning shape were critical to the tube precision. The microstructure and mechanical performance for the as-extruded TiBw/Ti-6Al-4V composite tubes were systematically investigated. After extrusion, the transverse section microstructure of the TiBw/Ti6Al4V composite tube remained quasi-continuous and the TiBw were rotated to align the extrusion direction. Moreover, the tensile strength and elongation reached 1240 MPa and 13.5%, resulting from dynamic recrystallization and whisker rotation.

In 2016 Material and Science Shufeng Li et al. [20] proposed Titanium matrix composites (TMCs) reinforced with in situ-formed TiC particles and TiB whiskers were prepared by reacting titanium and B4C via powder metallurgy and hot extrusion. The effect of the in situ-formed TiC–TiB hybrid reinforcements on the microstructure and mechanical behavior of the TMCs was investigated. TiB whiskers exhibited favorable alignment, orienting parallel to the deformation axis after hot extrusion, while TiC particles and TiB whiskers were distributed homogenously throughout the extruded composites. The synthesized TMCs with a 13.6% volume fraction of TiC–TiB hybrid reinforcements presented a σ_{UTS} of 1138 MPa, representing a 74% improvement compared to pure titanium, and retained an acceptable elongation of 2.6%.

In 2015 journal of Material Technology Bong Sun You et al. proposed the variation induced in the microstructural in homogeneity of AZ31 alloy subjected to indirect extrusion was studied using tool steel dies with angles of 30◦, 60◦and 90◦. Finite element modeling (FEM) of this extrusion process was also carried out to determine the metal flow, temperature evolution and effective strain distribution, which were then correlated with the observed microstructural changes. Although all extruded samples were found to have a bimodal microstructure consisting of equiaxed fine recrystallized (DRXed) grains and elongated coarse un DRXed grains, the inhomogeneity of their microstructural characteristics (i.e., DRX fraction and texture intensity) decreased in cross section with an increase in the die angle. The FEM analysis also demonstrated that a faster metal flow, higher temperature, and larger effective strain are generated in an alloy extruded with a 90◦die angle, and that this enhances DRX behavior during extrusion and ultimately results in a homogeneously DRXed microstructure.

III PROPOSED MODELLING

In present work we perform the similar FEM approach for titanium matrix composite billets with the help of numerical analysis predict the mechanical properties and validate with the existing experimental results of **Wang et al** and with the help of simulation we can also predict the Variation of punch load with punch travel at different friction factor.

The main objective of this proposed Modelling:

- Draw Fem Simulation 3d model for hot in-direct extrusion
- Validations with experimental data
- Punch load and Punch displacement
- Strength of billet
- FEM with different di angle

Modelling of the System

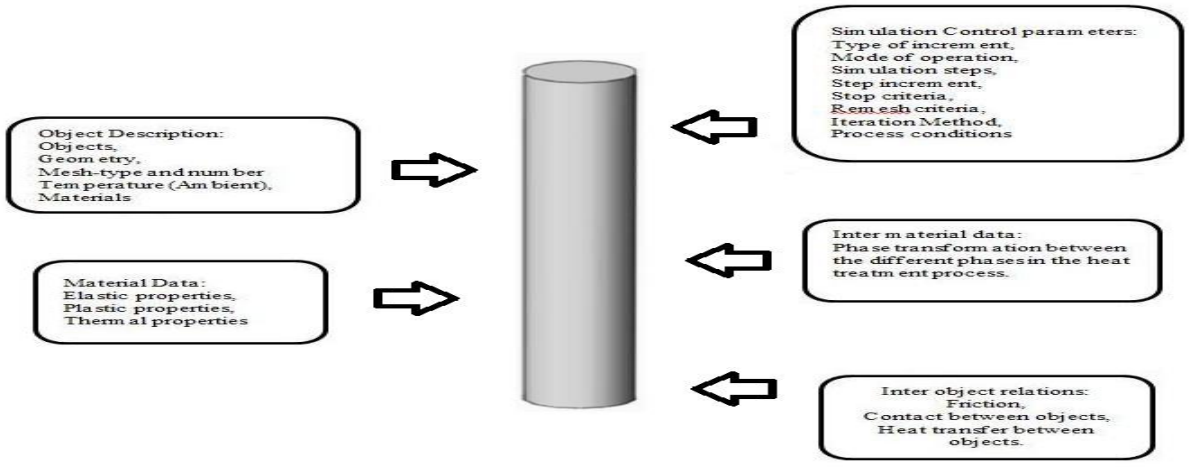

Figure 1 Major input parameters for FEM simulation

Simulation control

The SI unit convention with the Langrangian incremental type followed by a deformation mode is selected for the FEM simulation. The mechanical, thermal and phase transformations simulates the deformation into the work piece. Terminate the operation is performed when the specified distance is reached by the primary die and aborting distance are in combination with the reference points. The step size is the crucial for the simulation to perform the operation. The step size can be controlled by two ways either by die displacement or by time increment. The present simulation analysis is performed by controlling the time increment. During the simulation severe plastic deformation takes of the work piece (Slave). This Severe plastic deformation causes the work piece to distort which can be used further (negative Jacobean). The operation to be performing re-meshing after the mesh is distorted. The process of re-meshing is substituting the distorted mesh with a new mesh along with interpolating the field variables (strain, velocity, damage, and temperature, etc.) from old mesh to new mesh. The object re-meshing is performed to a slave (billet). The re-meshing depends on the interference between the primary die and the billet. The depth of interference is the depth an element edge of the slave object crosses the surface of a master object.

Simulation modelling

In finite element modelling (FEM), combined extrusion-forging and combined extrusion process technique is used to produce different types of collet chuck holders, at varying rate of ram displacements. The Non-linear-equations are solved with the help of direct iteration method and the Newton-Raphson method. Flow behavior was studied with, a modified Lagrangian method for the finite element code. The initial estimate of the Conjugate Gradient method, the direct iteration method is employed in the solution procedure, which is further used to find the velocity error and force error, obtained as 0.004 and 0.03 respectively. It has assumed that the billet was rigid plastic and the die, container, and flow guide is indeed rigid during the simulation process. The four-noded tetrahedron elements have been employed. In this finite element simulation, an isothermal process was adopted.

Simulation for the present problem

In the present CEF and CE processes a cylindrical billet made of Ti6Al4V alloy was selected as the matrix alloy, (chemical composition shown in Table 1) is forced by the punch, against the bottom die, which is stationary. Followed by extrusions in the various directions and filling in the radial orientation of the die cavity. The axis-symmetry 3d model extrusion die set-up.

Table 1 Chemical Composition of Different Material

material	composition					RF	TiB	TiC	Mole Ratio
	AIV	**AL**	**B4C**	**C**	**Ti**	**vol %**	**vol %**	**vol %**	**TiB:TiC**
Ti6Al4V	7.75	1.89	0.62	0.40	Bal.	5.0	2.6	2.4	1.1

A defined friction factor for the billet, die, container and flow guide interfaces has been set for the hot indirect extrusion condition. The four node tetrahedron elements have employed. A mesh independence test was performed to use ANSYS FEM the analyses to get the desired and accurate punch loads at various frictional conditions friction factor of 0.12, 0.18 and 0.37 which is calibrated at different ranges of elements (at ram velocity of 1.1 mm/min for first product as an illustration). The work piece is modelled using approximately 20000 meshing elements and 3489 nodes for the billet without hampering the accuracy of the final results.

Similar grid independence test were conducted at different ram velocities which has negligible effect. The temperature of all the objects is set to 35ºC. The process parameters assumed for the current analysis is discussed below. The flow stress is obtained from the experimental results during compression test. For the present finite element analysis, isothermal condition is assumed. Direct iteration method and Newton-Raphson methods have been adopted for solving the non-linear equations. A good initial guess has generated for the Newton-Raphson method using the direct iteration method, for the speedy final convergence. When the plastic deformation reaches the steady state, the simulation is stopped.

The assumptions made in the simulation process are as follows:

1. The material of die has taken as rigid
2. Ti6Al4V is taken as the billet in the simulation process and modelled using von Mises yield criterion for an isotropic rigid plastic material.
3. The friction factor for the interface work piece/die is considered as constant, which has found from ring test experimentally.
4. The billet axis has incorporated with the centroid of the die orifice.
5. Global re-meshing criterion and logarithmic interpolation.

For every friction condition three ram velocities are considered, these are:
i. 0.5 mm/min,
ii. 1.1 mm/min, and
iii. 2 mm/min.

IV NUMERICAL ANALYSIS

The method numerical analysis is carried out to get the final product from the initial cylindrical billet of 82 mm diameter and detail dimensions of the final product obtained is of 76 mm diameter and 50 mm length by compressing the round billet inside a rigid container with required cavity by a rigid punch to demonstrate the process of combined extrusion. The dies and punch plate used for simulation was same as that of experimental sets.

A defined friction factor for the billet, die, container and flow guide interfaces has been set for the hot indirect extrusion condition. The four node tetrahedron elements have employed. A mesh independence test was performed to use ANSYS FEM the analyses to get the desired and accurate punch loads at various frictional conditions friction factor of 0.12,0.18,0.37 which is calibrated at different ranges of elements (at ram velocity of different mm/min for first product as an illustration in figure 2 to 4).

Extrusion Load at different frictions and ram velocities

Variation of punch load with punch travel at friction factor of 0.12, 0.18, 0.37 at 45° Die angle

Figures 2 gives comparison of punch load with punch movement for different velocities using lubricant MoS2 + grease (60:40) with friction factor 0.12,0.18,0.37 and Die angle 45° and 100% grease and no lubrication respectively. The maximum extrusion loads at flashing are provided in Table 1. The ram displacement behaviors show that the total process can be assumed to consist of four stages:

- Initial stage, the load gradually increases backward extrusion takes place,
- Second stage, forward and lateral extrusion takes place,
- Combined stage, both extrusion and forging takes place for corner filling,
- The unsteady state stage, steep rise in load to form flash. As the metal flow are hindered, redundant work increases, subsequently the load increases unsteadily.

Table No. 1 for 45° Die angle

Sl. No.	Friction factor	Ram velocity (mm/min)	Peak load at flashing, kN
1	0.12	0.5	157.70
2		1.0	164.00
3		2.0	172.10
4	0.18	0.5	161.70
5		1.0	168.40
6		2.0	173.70
7	0.37	0.5	174.00
8		1.0	189.50
9		2.0	195.4

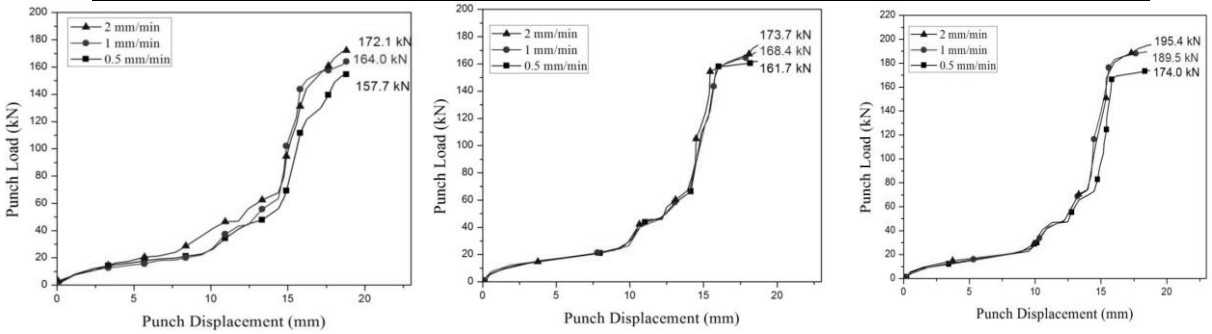

Figure 2 Variation of punch load with punch travel at friction factor of 0.12, 0.18, 0.37 at 45° Die angle

In the figures 2 gives comparison of punch load with punch movement for different velocities using lubricant MoS2 + grease (60:40) with friction factor 0.12,0.18,0.37 and Die angle 45° and 100% grease and no lubrication respectively. The maximum extrusion loads at flashing are provided in Table 4.1. It is evident from the Table 4.1 that with increase of friction the

load increases and also with ram velocity load requirements increases because of work hardening.

Variation of punch load with punch travel at friction factor of 0.12, 0.18, 0.37 at 60° Die angle

Figures 3 gives comparison of punch load with punch movement for different velocities using lubricant MoS2 + grease (60:40) with friction factor 0.12,0.18,0.37 and Die angle 60° and 100% grease and no lubrication respectively. The maximum extrusion loads at flashing are provided in Table 2. The ram displacement behaviors show that the total process can be assumed to consist of four stages:

- Initial stage, the load gradually increases backward extrusion takes place,
- Second stage, forward and lateral extrusion takes place,
- Combined stage, both extrusion and forging takes place for corner filling,
- The unsteady state stage, steep rise in load to form flash. As the metal flow are hindered, redundant work increases, subsequently the load increases unsteadily.

Table No. 2 for 60° Die angle

Sr. No.	Friction factor	Ram velocity	Peak load at flashing, kN
1	0.12	0.5	150.2
2		1.0	153.21
3		2.0	160.8
4	0.18	0.5	152.7
5		1.0	166.2
6		2.0	174.5
7	0.37	0.5	177.0
8		1.0	185.6
9		2.0	193.4

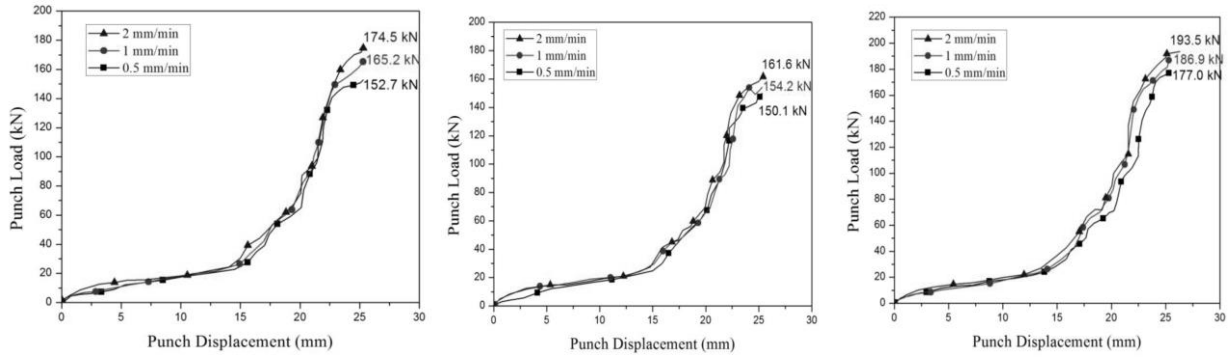

Figure 3 Variation of punch load with punch travel at friction factor of 0.12, 0.18, 0.37 at 60° Die angle

In the figures 3 gives comparison of punch load with punch movement for different velocities using lubricant MoS2 + grease (60:40) with friction factor 0.12,0.18,0.37 and Die angle 60° and 100% grease and no lubrication respectively. The maximum extrusion loads at flashing are provided in Table 2. It is evident from the Table 2 that with increase of friction the load increases and also with ram velocity load requirements increases because of work hardening.

Variation of punch load with punch travel at friction factor of 0.12, 0.18, 0.37 at 75° Die angle

Figures 4 gives comparison of punch load with punch movement for different velocities using lubricant MoS2 + grease (60:40) with friction factor 0.12,0.18,0.37 and Die angle 75° and 100% grease and no lubrication respectively. The maximum extrusion loads at flashing are provided in Table 3. The ram displacement behaviors show that the total process can be assumed to consist of four stages:

- Initial stage, the load gradually increases backward extrusion takes place,
- Second stage, forward and lateral extrusion takes place,
- Combined stage, both extrusion and forging takes place for corner filling,
- The unsteady state stage, steep rise in load to form flash. As the metal flow are hindered, redundant work increases, subsequently the load increases unsteadily.

Table No. 3 for 70° Die angle

Sr. No.	Friction factor	Ram velocity (mm/min)	Peak load at flashing, kN
1	0.12	0.5	143.6
2		1.0	146.2
3		2.0	153.7
4	0.18	0.5	142.3
5		1.0	155.2
6		2.0	156.6
7	0.37	0.5	151.2
8		1.0	163.8
9		2.0	178.4

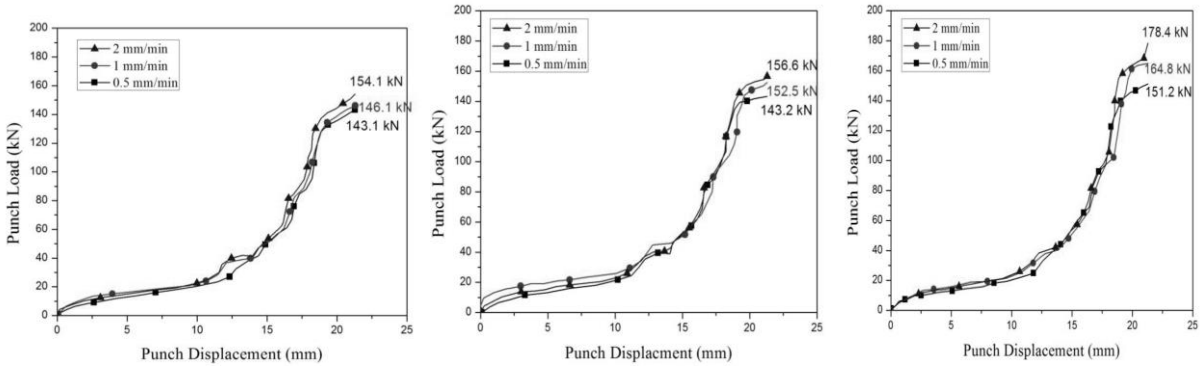

Figure 4 Variation of punch load with punch travel at friction factor of 0.12, 0.18, 0.37 at 75° Die angle

In the figures 4 gives comparison of punch load with punch movement for different velocities using lubricant MoS2 + grease (60:40) with friction factor 0.12,0.18,0.37 and Die angle 75° and 100% grease and no lubrication respectively. The maximum extrusion loads at flashing are provided in Table 4.3. It is evident from the Table 4.3 that with increase of friction the load increases and also with ram velocity load requirements increases because of work hardening.

Die Filling

In figure 5 shows the progressive change in shape of extrusion-forged product at different punch movements when the friction factor is 0.12 and the ram speed is 0.5 mm/min (as illustration). The die filling process substantiate that the total process can be thought of four stages as explained earlier, i.e., initial compression stage backward extrusion takes place during (0 - 10.0 mm of ram movement), in second stage during (10.0 - 16.0 mm ram) travel lateral extrusion takes place to form collar, during third stage (16.0 - 18.0 mm ram travel) corner filling and forward extrusion takes place, and in last stage (18.0 -18.3 mm ram travel) flash is formed to complete the process. It also explains that combined extrusion forging processes takes place simultaneously till the die cavity is completely filled, after which flash is started to form.

Metal flow pattern show the contour of displacements in both the horizontal and axial direction after 10.0 mm, 16.0 mm, 18.0 mm and 18.3 mm ram displacements respectively at 0.5 mm/min ram velocity with constant frictional conditions. Similarly, Figures above shows the contour of displacements in both the horizontal and axial direction after 10.0 mm, 16.0 mm, 18.0 mm and 18.3 mm ram displacements respectively with varying ram velocities at 0.13 frictional condition. The degree of distortion of gridlines at different stages confirms the load ram displacement behavior. Severe grid distortion at flashing stage validates the maximum load due to maximum redundant work. It is also seen that the whole billet, rather than part close to punch, is deforming simultaneously in different directions. Also, there is a non-uniform grid distortion due to friction at die-billet interface.

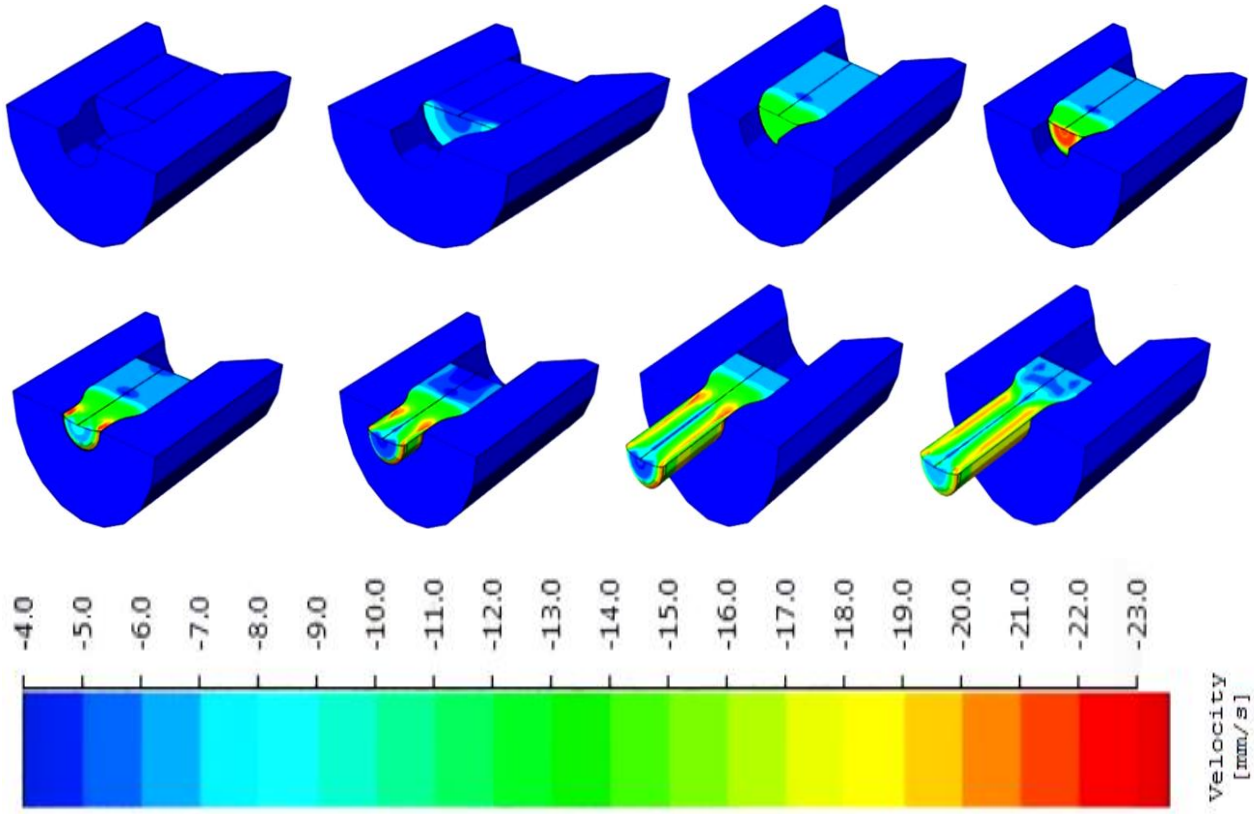

Figure 5 Different frame by frame images of a billetes coming out from the cavity with die angle 45 degree.

Validation FEM model

The simulation had also performed for different die angles and stress strain curve as shown figure 6 which is obtain from ANSYS.

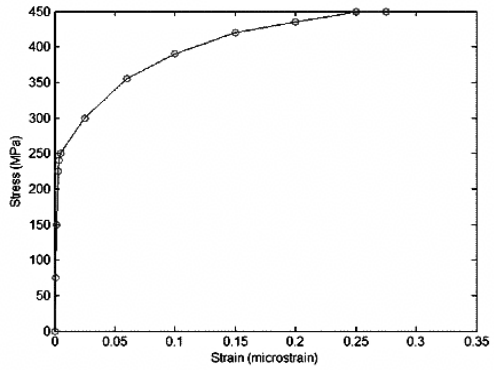

Figure 6 stress strain for Billet

The table 4 and 5 shows the comparison of experimental and FEM simulated results

Table No. 4 Experimental and FEM Simulated Results

Extrusion Angle	Experimental Tensile strength (N/mm^2)	Simulated Tensile strength (N/mm^2)	Percentage Error (%)
45	1082	1070.12	1.11
60	1068	1059.78	0.75
75	1062	1059.01	0.28

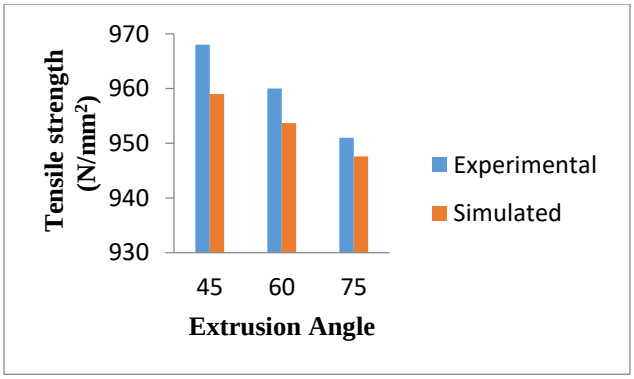

Figure 7 Comparison between Experimental and Simulated Results at Graph of Tensile Strength (N/mm^2)

Table No. 5 Experimental and FEM Simulated Results

Extrusion Angle	Experimental Yield strength (N/mm^2)	Simulated Yield strength (N/mm^2)	Percentage Error
45	968	959.01	0.92
60	960	953.70	0.66
75	951	947.59	0.36

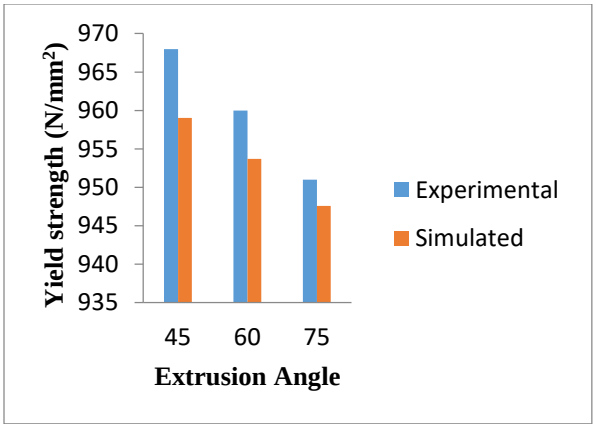

Figure 8 Comparison between Experimental and Simulated Results at Graph of Yield Strength (N/mm^2)

The results obtained can be summarized as in the present chapter the finite element analysis for three different types of dies were performed by simulation processes. Similar conditions of experimental analysis are taken into account for performing the present FEM analysis. Combination of three types of dies with frictional conditions. Different stages of deformation for 45 degree dies are performed for clear understating of die filling. Different stages of die filling data are used for further comparison analysis. Different stages of metal flow pattern for 45 degree dies are obtained for clear understanding of grain flow and shear effected regions. Shows the punch load and punch displacement variation.

V CONCLUSION

Simulations were carried out for the analysis of the Ti6Al4V composite were successfully indirect different extrusion angles of die in FEM processed (45°, 60° and75°).

- Initial compression stage, in which the load gradually increases, forms a small indentation hole by backward extrusion.
- Second stage, in which radial extrusion formation of billets are formed along with the forward extrusion of the part was performed, combined stage, corner die filling and extrusion of part was done,
- The unsteady state stage, in which there is a steep rise in load. In this stage, flash is formed, as the metal flow has hindered and controlled, the load increases unsteadily.

In case of third product metal flows out through the exit extrusion die present at the bottom, hence no flash provision is equipped.

The last product is manufactured by multi stage extrusion process in which the first product is the initial input specimen. Hence, the process is thought consists of two stages.

The results obtained can be summarized as below:

- In the present chapter the finite element analysis for three different types of dies were performed by simulation processes.
- Similar conditions of experimental analysis are taken into account for performing the present FEM analysis. Combination of three types of dies with frictional conditions
- Different stages of deformation for 45 degree dies are performed for clear understating of die filling. Different stages of die filling data are used for further comparison analysis.
- Different stages of metal flow pattern for 45 degree dies are obtained for clear understanding of grain flow and shear effected regions.
- Shows the punch load and punch displacement variation

REFERENCES

1) Mohamed A. Taha, “Practicalization of cast metal matrix composites (MMCCs)”, Materials and Design, 22 (2001), 431-441.
2) Bekir Sadık Unlu, “Investigation of tribological and mechanical properties Al2O3–SiC reinforced Al composites manufactured by casting or P/M method”, Materials and Design, 29 (2008), 2002–2008.
3) Ahmet Hascalik and Nuri Orhan, “Effect of particle size on the friction welding of Al2O3 reinforced 6061Al alloy composite and SAE 1020 steel”, Materials and Design, 28 (2007), 313–317.
4) Fevzi Bedir, “Characteristic properties of Al–Cu–SiCp and Al–Cu–B4Cp composites produced by hot pressing method under nitrogen atmosphere”, Materials and Design, 28 (2007), 1238–1244.
5) Halil Arik, “Effect of mechanical alloying process on mechanical properties of a-Si3N4 reinforced aluminum-based composite materials”, Materials and Design, 29 (2008), 1856–1861.
6) Hideki Sekine and Rong Chent, “A combined microstructure strengthening analysis of SiCp/Al

metal matrix composites", Composites, 26 (1995) 183- 188.

7) Recep Ekici, M. Kemal Apalak , Mustafa Yıldırım , Fehmi Nair, "Effects of random particle dispersion and size on the indentation behavior of SiC particle reinforced metal matrix composites", Materials and Design, 31 (2010) , 2818–2833.
8) D.K. Dwivedi, "Adhesive wear behaviour of cast Aluminum–silicon alloys: Overview", Materials and Design, 31 (2010), 2517–2531.
9) Madeva Nagaral, V Auradi, S. A. Kori, "Dry sliding wear behavior of graphite particulate reinforced Al6061 alloy composite materials", Applied Mechanics and Materials, 592-594 (2014), 170-174.
10) S.M. Seyed Reihani, "Processing of squeeze cast Al6061–30vol% SiC composites and their characterization", Materials and Design, 27 (2006), 216–222.
11) Rasit Koker, Necat Altinkok, Adem Demir, "Neural network based prediction of mechanical properties of particulate reinforced metal matrix composites using various training algorithms", Materials and Design, 28 (2007), 616–627.
12) C. Santosa, S. Ribeiro, K. Strecker, D. Rodrigues Jr. , C.R.M. Silva, "Highly dense Si3N4 crucibles used for Al casting: An investigation of the aluminum–ceramic interface at high temperatures", Journal of Materials Processing Technology, 184 (2007), 108–114.
13) B. Abbasipour, B. niroumand, S. M. Monir, "Compo-casting of A356-CNT composite", Trans. Nonferrous Met. Soc. China, 20(2010), 1561−1566.
14) Rupa Dasgupta, "Aluminum alloy-based metal matrix composites: A potential material for wear resistant applications", International Scholarly Research Network ISRN Metallurgy Volume 2012, Article ID 594573, 14 pages doi:10.5402/2012/594573.
15) G. G. Sozhamannan, S. Balasivanandha Prabu, V. S. K. Venkatagalapathy, "Effect of Processing Parameters on Metal Matrix Composites: Stir Casting Process", Journal of Surface Engineered Materials and Advanced Technology, 2012, 2, 11-15.
16) Madeva Nagaral, Bharath V and V Auradi, "Effect of Al2O3 particles on mechanical and wear properties of 6061Al alloy metal matrix composites", Journal of Material Science and Engineering, 2013, 2:1, doi:10.4172/2169-0022.1000120.
17) D. Brabazon, D.J. Browne, A.J. Carr, "Mechanical stir casting of Aluminum alloys from the mushy state: process, microstructure and mechanical properties", Materials Science and Engineering A, 326 (2002), 370- 381.
18) Guangfa Huang, Xian glong Guo,Yuan fei Han , Liqiang Wang, Weijie Lu, "Effect of extrusion dies angle on the micro structure and properties of (TiB+TiC)/Ti6Al4V in situ titanium matrix composite" , Material and Science Engineering 2016.
19) Jian lei Yang, Xueyan Jiao, Wenzhen Chen, Wencong Zhang and Guofeng Wang, "A Novel Extrusion for Manufacturing TiBw/Ti6Al4V Composite Tubes with a Quasi-Continuous Reinforced Structure", Material 2017.
20) Shufeng Li, Katsuyoshi Kondoh, Hisashi Imai, Biao Chen, Lei Jia, Junko Umeda, Yabo Fu, "Strengthening behavior of in situ-synthesized (TiC–TiB)/Ti composites by powder metallurgy and hot extrusion", Material and Design 2016.
21) Bong Sun You et al, "Die angle dependency of microstructural inhomogeneity in an indirect-extruded AZ31 magnesium alloy", Journal of Material Technology 2015.
22) Yuan fei Han, Jiu xiao Li, Guangfa Huang, Yuting Lv, Xi Shao, Weijie Lu, Di Zhang, "Effect of ECAP numbers on microstructure and properties of titanium matrix composite" Material and Design 2015.
23) Yang Yu, Wencong Zhang, Wenqian Dong, Jianlei Yang, Yangju Feng, "Effects of pre-sintering on microstructure and properties of TiBw/Ti6Al4V composites fabricated by hot extrusion with steel cup", Material and Science Engineering 2015.